DOI: 10.1002/asia.200800070

VIP

Polymorphs and Polymorphic Cocrystals of Temozolomide

N. Jagadeesh Babu, L. Sreenivas Reddy, Srinivasulu Aitipamula, and Ashwini Nangia*[a]

Abstract: Crystal polymorphism in the antitumor drug temozolomide (TMZ), cocrystals of TMZ with 4,4′-bipyridine-*N*,*N*′-dioxide (BPNO), and solid-state stability were studied. Apart from a known X-ray crystal structure of TMZ (form 1), two new crystalline modifications, forms 2 and 3, were obtained during attempted cocrystallization with carbamazepine and 3-hydroxypyridine-*N*-oxide. Conformers A and B of the drug molecule are stabilized by intramolecular amide N–H···$N_{imidazole}$ and N–H···$N_{tetrazine}$ interactions. The stable conformer A is present in forms 1 and 2, whereas both conformers crystallized in form 3. Preparation of polymorphic cocrystals I and II (TMZ·BPNO 1:0.5 and 2:1) were optimized by using solution crystallization and grinding methods. The metastable nature of polymorph 2 and cocrystal II is ascribed to unused hydrogen-bond donors/acceptors in the crystal structure. The intramolecularly bonded amide N–H donor in the less stable structure makes additional intermolecular bonds with the tetrazine C=O group and the imidazole N atom in stable polymorph 1 and cocrystal I, respectively. All available hydrogen-bond donors and acceptors are used to make intermolecular hydrogen bonds in the stable crystalline form. Synthon polymorphism and crystal stability are discussed in terms of hydrogen-bond reorganization.

Keywords: cocrystallization · crystal engineering · hydrogen bonds · polymorphism · supramolecular synthons

Introduction

Polymorphs[1] and cocrystals[2] are solid-state forms of compounds used in pharmaceutical formulation, drug-life-cycle management, and patenting.[3] The design and synthesis of cocrystals[4] by supramolecular-synthon strategies[5] is an important activity in crystal engineering. Temozolomide (8-carbamoyl-3-methylimidazo[5,1-*d*]-1,2,3,5-tetrazin-4(3*H*)-one, TMZ) is an antitumor prodrug against malignant melanoma that acts by water-assisted tetrazinone ring opening and DNA alkylation of the incipient cytotoxic form. Only one crystal structure of TMZ has been reported;[6] it belongs in the space group $P2_1/c$ with unit-cell parameters $a=17.332(3)$, $b=7.351(2)$, $c=13.247(1)$ Å, $\beta=109.56(1)°$. Nine unsolvated TMZ polymorphs were disclosed in a recent US patent.[7] However, the structural origins of polymorphism in TMZ are not known because the various polymorphic forms were characterized and differentiated by powder X-ray diffraction (PXRD) and IR spectroscopy. Accurate information about hydrogen bonding and molecular packing in crystal structures is only available by single-crystal X-ray diffraction.

Temozolomide has a more complex molecular structure than pyrazinamide and isonicotinamide (Scheme 1). The presence of carboxamide and N-heterocycle functional

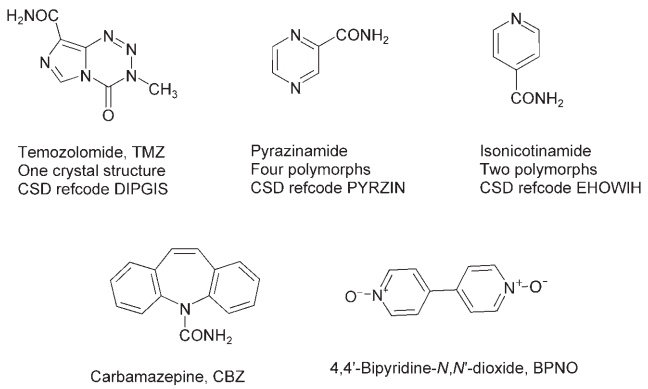

Scheme 1. Comparison of the molecular structure of temozolomide with those of pyrazinamide and isonicotinamide. There are more heterocycle N acceptor atoms for the amide group in TMZ. CBZ and BPNO are the cocrystal formers used in this study.

[a] N. J. Babu, L. S. Reddy, S. Aitipamula, Prof. Dr. A. Nangia
School of Chemistry
University of Hyderabad
Hyderabad 500 046 (India)
Fax: (+91) 40-2301-0567
E-mail: ashwini.nangia@gmail.com

Supporting information for this article is available on the WWW under http://dx.doi.org/10.1002/asia.200800070.

groups in the same molecule is believed to be a favorable structural feature for polymorphism and cocrystal formation because of the possibility for N–H···N hydrogen bonding as well as the usual N–H···O hydrogen bonds of the amide group. For example, dimorphs of isonicotinamide and tetramorphs of pyrazinamide display differences in N–H···O and N–H···N hydrogen-bond synthons.[8] The Cambridge Structural Database (CSD)[9] refcode identifiers of these compounds are given in Scheme 1. Cocrystals of both pyrazinamide and isonicotinamide have been prepared with suitable cocrystal formers (CCFs).[10] The presence of tetrazine, imidazole, and amide groups in temozolomide suggests that crystallization experiments should yield polymorphs and cocrystals of this important drug mediated through N–H···O and several potential N–H···N hydrogen bonds. Herein, X-ray crystal structures of two new polymorphs of temozolomide and polymorphic cocrystals with 4,4′-bipyridine-*N*,*N*′-dioxide (BPNO) are analyzed as hydrogen-bonded or synthon polymorphs.

Abstract in Telugu:

కణతనిరోధక మందు అయిన టిమొజోలమైడ్(టిఎమ్జెడ్) యొక్క బహురూపాంతరాలు, 4,4-బైపిరిడిన్-N,N'-డైఆక్సైడ్(బిపిఎన్ఒ) తో టిఎమ్జెడ్ యొక్క సహస్ఫటికాలు మరియు ఘనస్థితిలో వాటి స్థిరత్వాన్ని చెప్పడం జరిగింది. ముందుగా తెలిసినటువంటి టిఎమ్జెడ్ యొక్క ఎక్సరే స్ఫటిక నిర్మాణము 1 కాకుండా, కొత్త టిఎమ్జెడ్ రూపాలు 2 మరియు 3లు కార్బమజపిన్ మరియు 3-హైడ్రాక్సీ పిరిడిన్ N -ఆక్సైడ్ తో సహస్ఫటికీకరణ పద్ధతి ద్వారా ఏర్పడ్డాయి. టిఎమ్జెడ్ యొక్క ప్రాదేశికాలు A మరియు B, అణ్వంతర ఎమైడ్ N-H...N(ఇమిడజోల్) మరియు N-H...N(టెట్రజీన్) సహచర్యం వలన స్థిరత్వం పొందినవి. స్థిరప్రాదేశికం A రూపం 1 మరియు 2లో ఉంటుంది. కాని ఈ రెండు ప్రాదేశికాలు రూపం 3లో స్ఫటికీకరణం చెందుతాయి. ద్రావణం నుంచి స్ఫటికీకరణం, నూరుట పద్ధతుల ద్వారా ఏర్పడిన బహురూపాంతర సహస్ఫటికాలు I మరియు II (టిఎమ్జెడ్.బిపిఎన్ఒ 1:0.5 మరియు 2:1) తయారీని స్థిరీకరించడం జరిగింది. స్ఫటికనిర్మాణంలో దాత, గ్రహీతల మధ్య బంధాలు లేకపోవడం వల్ల, టిఎమ్జెడ్ రూపం 2, దాని సహస్ఫటికం II తక్కువ స్థిరత్వాన్ని కలిగివున్నవని చెప్పవచ్చును. ఎమైడ్ యాంటీ N-H దాత తక్కువ స్థిరత్వం కలిగిన నిర్మాణంలో స్వేచ్ఛాయుతంగా వుంటుంది. ఇది స్థిర రూపాంతరం 1 మరియు సహస్ఫటికము I లోని టెట్రజీన్ C=O మరియు ఇమిడజోల్ N గ్రహీతలతో హైడ్రోజన్ బంధం ఏర్పడుతుంది. అయితే అన్ని స్ఫటిక నిర్మాణాలలో సిన్ N-H...O హైడ్రోజన్ బంధాలు కలిగివున్నవని చెప్పవచ్చు. స్థిరస్ఫటిక రూపంలో అన్ని హైడ్రోజన్ బంధ దాత, గ్రహీతలు ఉపయోగపడేవిధంగా లభ్యమయినవి. హైడ్రోజన్ బంధ పునఃస్థాపన ద్వారా సింథాన్ రూపాంతరం మరియు స్ఫటిక స్థిరత్వాన్ని వివరించవచ్చును.

Results and Discussion

TMZ Polymorphs

Crystallization of TMZ from common solvents such as EtOH, *i*PrOH, acetone, and CH_3CN by slow evaporation gave single crystals that matched with the unit cell of form 1 reported at room temperature (CSD refcode DIPGIS10).[6] Reflections were collected at 100 K for better comparison with structural data in this study. TMZ polymorphs 2 and 3 were obtained during attempted cocrystallization with carbamazepine (CBZ) and pyridine-*N*-oxide partners (see Experimental Section).

Form 1

This form crystallizes in the space group $P2_1/c$ (Table 1) with two symmetry-independent molecules ($Z'=2$). Both molecules adopt conformation A, which has an intramolecular N_{amide}–H···$N_{imidazole}$ bond to form a five-membered ring (Scheme 2). The crystallographic definition of Z' is the number of formula units in the unit cell (Z) divided by the number of independent general positions for that space group.[11] Chemically speaking, Z' is the number of crystallographically unique molecules or conformers that tessellate in space to build the crystal structure. TMZ molecules undergo hydrogen bonding in the crystal structure through the amide dimer synthon (N1–H1A···O3: 2.03 and 3.024(2) Å, 167.7°; N7–H7A···O1: 1.84 and 2.855(2) Å, 177.3°; D–H···A measurements are given as H···A and D···A distances (Å) and D–H···A hydrogen-bond angle (°)) and extend as helices down the [010] direction through N7–H7B···O4 (2.02 and 2.997(2) Å, 160.7°) and C6–H6B···O1 (2.28 and 3.279(2) Å, 151.5°) H bonds (Figure 1). Weak C–H···O, N–H···N, and C–H···N interactions (Table 2) complete the crystal packing.

Form 2

Cocrystallization of TMZ with CBZ or 3-hydroxypyridine-*N*-oxide, with the intent of obtaining a 1:1 cocrystal, gave a second polymorph of TMZ of the space group $P2_1/n$ with conformation A ($Z'=1$). The amide dimer between inversion-related TMZ molecules (N1–H1A···O1: 1.84 and 2.848(1) Å, 170.1°) extends via C4–H4···O2 (2.14 and 3.208(1) Å, 165.0°) dimers as a one-dimensional tape parallel to the [120] direction (Figure 2). There are helices of C6–H6A···O1 (2.42 and 3.442(1) Å, 155.3°) and C6–H6B···N2 (2.61 and 3.276(1) Å, 118.8°) interactions. Surprisingly, the amide a*nti* N–H moiety is not involved in conventional intermolecular hydrogen bonds in this crystal structure.

Form 3

Cocrystallization of TMZ and CBZ gave blocklike crystals that matched with the above two monoclinic crystal structures (same unit-cell parameters) and a few crystals with irregular morphology. This latter crystal was found to be a third polymorph of TMZ. There are now two conformers, A and B ($Z'=2$; Scheme 2), in the space group $P\bar{1}$. The amide

Table 1. X-ray crystal-structure data of TMZ polymorphs and cocrystals.

	TMZ form 1	TMZ form 2	TMZ form 3	TMZ·BPNO cocrystal I (1:0.5)	TMZ·BPNO cocrystal II (2:1)	TMZ·BPNO cocrystal III (1:1)
Empirical formula	$C_6H_6N_6O_2$	$C_6H_6N_6O_2$	$C_6H_6N_6O_2$	$(C_6H_6N_6O_6)\cdot 0.5\,(C_{10}H_8N_2O_2)$	$2\,(C_6H_6N_6O_6)\cdot 1\,(C_{10}H_8N_2O_2)$	$(C_6H_6N_6O_6)\cdot(C_{10}H_8N_2O_2)$
M_r	194.17	194.17	194.17	576.52	576.52	382.35
Crystal system	monoclinic	monoclinic	triclinic	triclinic	monoclinic	orthorhombic
Space group	$P2_1/c$	$P2_1/n$	$P\bar{1}$	$P\bar{1}$	$P2_1/c$	$P2_12_12_1$
T [K]	100(2)	100(2)	293(2)	100(2)	100(2)	100(2)
a [Å]	17.2127(11)	6.8218(5)	8.500(2)	7.7599(8)	6.6957(5)	6.6838(15)
b [Å]	7.2061(5)	7.4881(6)	10.004(3)	8.7874(9)	9.6801(7)	10.035(2)
c [Å]	13.1651(8)	15.6303(12)	11.309(3)	9.8737(11)	37.654(3)	24.051(6)
α [°]	90	90	99.270(4)	68.754(2)	90	90
β [°]	108.868(1)	96.5340(10)	108.857(5)	74.454(2)	95.510(2)	90
γ [°]	90	90	109.192(5)	89.719(2)	90	90
Z	8	4	4	1	4	4
V [Å^3]	1545.21(17)	793.25(11)	820.1(4)	601.37(11)	2429.3(3)	1613.1(6)
ρ_{calcd} [g cm^{-3}]	1.669	1.626	1.573	1.592	1.576	1.574
μ [mm^{-1}]	0.132	0.129	0.125	0.122	0.121	0.119
Reflns. collected	15132	4173	8304	4532	24686	16058
Unique reflns.	2977	1560	3129	2115	4799	1816
Observed reflns.	2451	1428	1530	1892	4172	1542
$R1$ ($I>2\sigma(I)$)	0.0407	0.0366	0.0617	0.0435	0.0399	0.0719
$wR2$ (all)	0.0916	0.0903	0.0948	0.1129	0.1012	0.1329
GOF	1.020	1.050	0.948	1.042	1.043	1.126

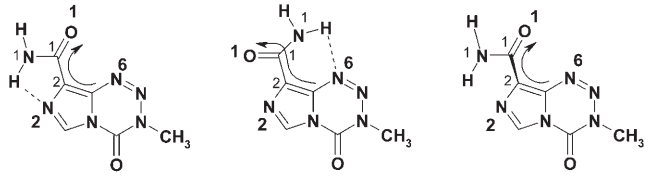

Scheme 2. Conformers A, B, and C of TMZ. Conformer A (N–H···$N_{imidazole}$ bond in a five-membered ring) was taken from the X-ray structure of form 1, and conformer B (N–H···$N_{tetrazine}$ bond in a six-membered ring) was extracted from form 3. The putative conformer C (perpendicular amide group) was generated computationally. Conformer energies are listed in Table 3.

group flips over to make an intramolecular N_{amide}–H···$N_{tetrazine}$ bond in conformer B (six-membered ring). Although $Z'=2$ in both crystal forms 1 and 3, the two crystallographically unique molecules have the same conformation in the former case ($\tau=-0.5$, $-3.5°$) but different conformations in this latter crystal structure ($\tau=5.1$, $178.3°$). The presence of different conformers of the same molecule in crystal structures, or conformational isomorphism due to $Z'>1$, is an interesting chemical occurrence that is as such not so common among polymorphic sets.[12] The amide dimer between conformers A and B (N1–H1A···O3: 2.11 and 3.114(4) Å, 169.3°; N7–H7A···O1: 1.86 and 2.863(5) Å, 171.7°) extends as 1D tapes through the C6–H6A···O4 interaction (2.44 and 2.989(5) Å, 109.4°), as shown in Figure 3. Such parallel tapes are connected by the N1–H1B···N8 (1.98 and 2.986(5) Å, 174.0°) and C4–H4···O2 dimers (2.27 and 3.327(5) Å, 164.6°) to form a 2D layer. Hydrogen-bonding differences in the polymorphs will be discussed later. Monoclinic forms 1 and 2 are helical structures whereas, triclinic form 3 is layered. The serendipitous discovery of new polymorphs during attempted cocrystallization is not totally surprising.[13] We did not isolate any cocrystals in the above-mentioned experiments.

Powder X-ray Diffraction

The known form 1 ($P2_1/c$)[6] was found to be identical with a patented form III.[7] PXRD of form 2 ($P2_1/n$) compares well with form IX of the same patent. That study provided an X-ray crystal structure of TMZ form IX for which only PXRD lines were reported.[7] Form 3, however ($P\bar{1}$), was not reported in that study (see Supporting Information, Figures S1 and S2 for PXRD plots). We refer to these polymorphs as forms 1–3.

Energy Relationships

It is difficult to measure the melting points of forms 1 and 2 (as an indicator of solid-form stability) because these compounds decompose upon heating. The crystal density (ρ_{calcd}) follows the order form 1 > form 2 > form 3 (1.669, 1.626, 1.573 g cm^{-3}). The original form 1 is the most stable polymorph according to the density rule.[14] Lattice-energy calculations (Cerius^2, COMPASS) are consistent with form 1 as the stable polymorph (-33.19 kcal mol^{-1}), followed by form 2 (-32.04 kcal mol^{-1}). The metastable nature of form 2 is ascribed to hydrogen-bonding differences in the two crystal structures. The amide *syn* NH moiety forms N–H···O hydrogen bonds in both structures. The *anti* NH moiety forms N–H···N hydrogen bonds in form 1, whereas the donor is not intermolecularly H-bonded in form 2 (Table 2 and Figures 1 and 2). Form 3 crystals of TMZ obtained in an earlier experiment could not be reproduced in subsequent batches.

CHEMISTRY
AN ASIAN JOURNAL

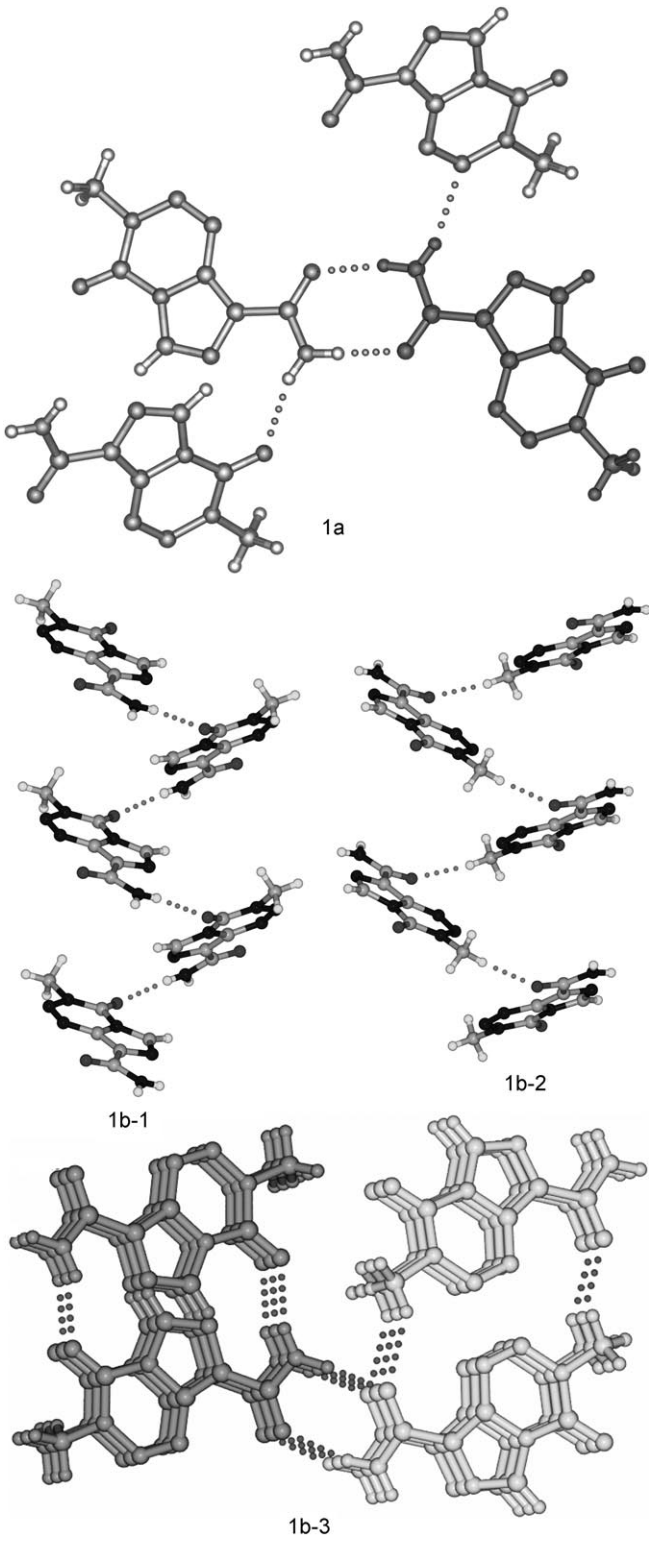

Figure 1. a) The carboxamide dimer of crystallographically unique molecules (shaded differently) in TMZ form 1. The *anti* NH moieties are involved in the N7−H7B···O4 and N1−H1B···N11 bonds. b) Helices mediated by N−H···O and C−H···O hydrogen bonds along the *b* axis are connected by the amide dimer of symmetry-independent molecules.

Table 2. Hydrogen-bond distances and angle parameters with neutron-normalized N–H, O–H, and C–H distances.

Crystal structure	Interaction	H···A [Å]	D···A [Å]	D−H···A [°]	Symmetry code
TMZ form 1	*syn* N1−H1A···O3 (amide C=O)	2.03	3.024(2)	167.7	$-1+x, y, -1+z$
	anti N1−H1B···N2 (imidazole N)[a]	2.44	2.804(2)	100.2	–
	anti N1−H1B···N11 (tetrazine N)	2.47	3.393(2)	150.7	$1-x, -1/2+y, 3/2-z$
	syn N7−H7A···O1 (amide C=O)	1.84	2.855(2)	177.3	$-1+x, y, -1+z$
	anti N7-H7B···N8 (imidazole N)[a]	2.35	2.746(2)	101.6	–
	anti N7−-H7B···O4 (tetrazine C=O)	2.02	2.997(2)	160.7	$2-x, -1/2+y, 3/2-z$
	C4−H4···N5	2.46	3.519(2)	163.4	$x, 1/2-y, 1/2+z$
	C4−H4···N6	2.32	3.327(2)	152.6	$x, 1/2-y, 1/2+z$
	C6−H6A···N2	2.78	3.523(3)	125.9	$1-x,1-y,1-z$
	C6−H6B···O1	2.28	3.279(2)	151.5	$1-x, -1/2+y, 1/2-z$
	C6−H6C···O4	2.70	3.402(2)	122.1	$x, -1+y, z$
	C10−H10···O3	2.48	3.104(2)	115.2	$x, 3/2-y, -1/2+z$
	C10−H10···N12	2.45	3.487(2)	159.0	$x, 3/2-y, -1/2+z$
	C12−H12B···N2	2.46	3.288(2)	131.8	$1-x, 1/2+y, 3/2-z$
TMZ form 2	*syn* N1−H1A···O1 (amide C=O)	1.84	2.848(1)	170.1	$-x, 2-y, -z$
	anti N1−H1B···N2 (imidazole N)[a]	2.25	2.804(1)	107.1	–
	C4−H4···O2	2.14	3.208(1)	165.0	$2-x, 1-y, -z$
	C6−H6A···O1	2.42	3.442(1)	155.3	$3/2-x, -1/2+y, 1/2+y$
	C6−H6A···N6	2.76	3.524(2)	126.8	$1+x, y, z$
	C6−H6B···O2	2.69	3.302(1)	115.3	$5/2-x, 1/2+y, 1/2-z$
	C6−H6B···N2	2.61	3.276(1)	118.8	$1/2+x, 1/2-y, 1/2+z$
	C6−H6C···O1	2.65	3.375(1)	124.1	$1+x, y, z$
TMZ form 3	*syn* N1−H1A···O3 (amide C=O)	2.11	3.114(4)	169.3	$-x, 1-y, -z$
	anti N1-H1B···N2 (imidazole N)[a]	2.71	2.861(5)	87.9	–
	anti N1−H1B···N8 (imidazole N)	1.98	2.986(5)	174.0	$x, y, -1+z$
	syn N7−H7A···O1 (amide C=O)	1.86	2.863(5)	171.7	$-x, 1-y, -z$
	anti N7−H7B···N12 (tetrazine N)[a]	2.29	3.036(5)	129.2	–
	anti N7−H7B···N11 (tetrazine N)	2.58	3.398(4)	137.0	$-x, 1-y, -z$
	C4−H4···O2	2.27	3.327(5)	164.6	$1-x, -y, -z$
	C6−H6A···O4	2.44	2.989(5)	109.4	$1-x, -y, 1-z$
	C6−H6C···O3	2.49	3.476(5)	151.4	$1+x, y, z$
	C12−H12B···O1	2.44	3.136(4)	120.6	$x, -1+y, z$

Table 2. (Continued)

Crystal structure	Interaction	H···A [Å]	D···A [Å]	D−H···A [°]	Symmetry code
TMZ·BPNO cocrystal I (1:0.5)	*syn* N1−H1A···O2 (tetrazine C=O)	2.10	3.085(2)	164.4	$x, y, 1+z$
	anti N1−-H1B···N2 (imidazole N)[a]	2.44	2.812(2)	100.8	–
	anti N1−H1B···N2 (imidazole N)	2.10	2.996(2)	145.8	$1-x, -y, -z$
	C4−H4···O2	2.33	3.398(2)	166.4	$1-x, -y, 1-z$
	C6−H6B···O3	2.31	3.077(2)	126.2	x, y, z
	C6−H6C···O2	2.80	3.710(2)	140.7	$1-x, 1-y, 1-z$
	C7−H7···O3	2.03	3.092(2)	165.6	$-x, 2-y, 1-z$
	C8−H8···N5	2.74	3.830(2)	178.5	$x, y, -1+z$
	C10−H10···N5	2.53	3.591(2)	166.2	$x, y, -1+z$
	C10−H10···N6	2.47	3.344(2)	136.9	$x, y, -1+z$
	C11−H11···O1	2.18	3.230(2)	160.4	$x, y, -1+z$
TMZ·BPNO cocrystal II (2:1)	*syn* N1−H1A···O6 (pyridine-*N*-oxide)	1.81	2.826(1)	177.0	$1-x, -1/2+y, 3/2-z$
	anti N1−-H1B···N2 (imidazole N)[a]	2.42	2.790(2)	100.5	–
	syn N7−H7A···O5 (pyridine-*N*-oxide)	1.84	2.851(2)	171.9	$2-x, -y, 2-z$
	anti N7-H7B···N8 (imidazole N)[a]	2.38	2.789(2)	102.9	–
	anti N1−H1B···O6 (pyridine-*N*-oxide)	2.47	3.375(1)	147.7	$-1+x, y, z$
	C4−H4···O4	2.18	3.199(1)	155.4	x, y, z
	C6−H6C···O5	2.49	3.468(2)	148.4	$2-x, 1-y, 2-z$
	C10−H10···O2	2.14	3.156(1)	154.0	x, y, z
	C13−H13···N6	2.50	3.458(2)	146.0	$1+x, -1+y, z$
	C14−H14···O1	2.06	3.129(1)	168.5	$1+x, -1+y, z$
	C16−H16···O3	2.02	3.126(1)	166.5	$x, 1+y, z$
	C17−H17···O5	2.29	3.275(2)	149.7	$2-x, 1-y, 2-z$
	C19−H19···O1	2.31	3.396(1)	173.8	$1+x, -1+y, z$
	C21−H21···O3	2.33	3.387(1)	164.7	$x, 1+y, z$
	C22−H22···N11	2.49	3.543(2)	162.4	$x, 1+y, z$
	C22−H22···N12	2.49	3.345(2)	134.5	$x, 1+y, z$
TMZ·BPNO cocrystal III (1:1)	*syn* N1−H1A···O3 (pyridine-*N*-oxide)	1.86	2.857(6)	167.2	$1/2+x, -1/2-y, -z$
	anti N1−H1B···N2 (imidazole N)[a]	2.35	2.764(7)	103.1	–
	C4−H4···O4	2.00	3.086(6)	173.6	$1-x, -1/2+y, 1/2-z$
	C6−H6A···O3	2.42	3.500(7)	170.5	$1+x, 1+y, z$
	C7−H7···O4	2.11	3.195(7)	173.5	$x, -1+y, z$
	C8−H8···O2	2.21	3.256(6)	161.4	$1-x, 1/2+y, 1/2-z$
	C11−H11···N5	2.42	3.362(7)	144.0	$-1/2+x, 1/2-y, -z$
	C12−H12···O3	2.17	3.240(7)	167.8	$x, -1+y, z$
	C13−H13···O1	2.12	3.116(6)	150.5	$-1/2+x, 1/2-y, -z$

[a] Intramolecular hydrogen bond.

The disappearing nature[15] of crystal form 3 is due to destabilization from strained conformer B, which is 1.44 kcal mol^{-1} higher in energy than conformer A, as calculated with Gaussian 03 (DFT, B3LYP/6-31G(d,p); Table 3). Conformer energies were calculated by fixing the main torsion angles to the experimental values while allowing bond distances to relax at the nearest local minima. The difference in the energy of the A and B conformers is due to electrostatics. The electron densities at the imidazole and tetrazine N atoms (N2 and N6) flanking the amide group are quite different. Electrostatic surface potential (ESP) charges at the electronegative N atoms were computed in the putative perpendicular amide conformation C (Scheme 2) because intramolecular H bonding lowers the negative potential at the acceptor N atoms by about 20 kcal mol^{-1} (compare the ESP charge at the same N atom in conformers A and B vs. C; Table 3). The electrostatic potential at the imidazole N2 atom is greater than the tetrazine N6 atom in conformer C

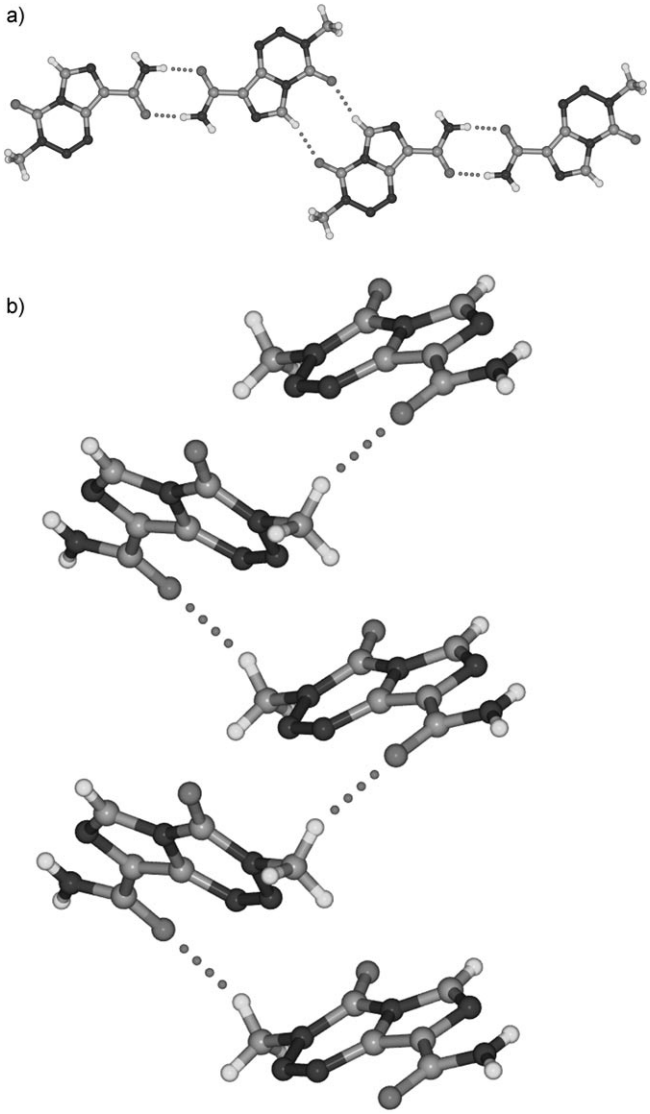

Figure 2. a) N−H···O and C−H···O dimers assemble in a tape motif in form 2. The *anti* NH moiety of $CONH_2$ makes only intramolecular hydrogen bonds in this crystal structure. b) Helical arrangement of TMZ through C6−H6A···O1 interaction along the *b* axis.

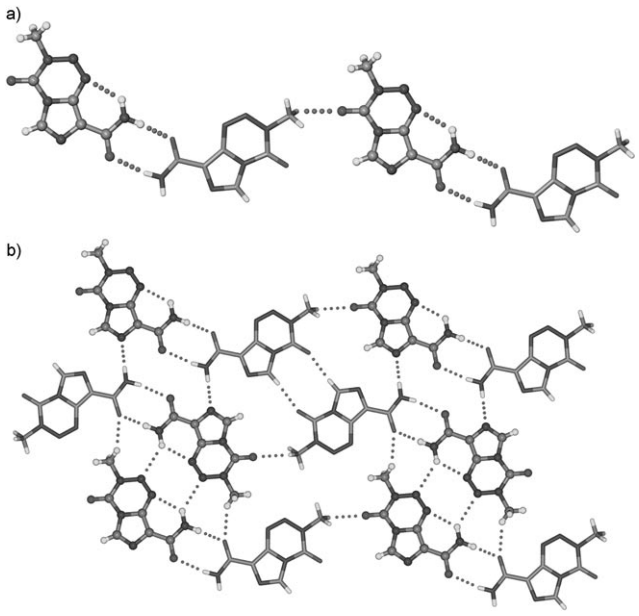

Figure 3. a) Amide N–H···O dimer of conformers A and B (capped-stick and ball-and-stick models). b) N–H···O and C–H···O dimers extend the 1D tapes into 2D sheets in form 3.

Table 3. Conformer energies and ESP charges.[a]

Conformer	E_{conf} [kcal mol^{-1}]	N2–C2–C1–N1 (τ) [°]	ESP charge N2 (imidazole) [kcal mol^{-1}]	ESP charge N6 (tetrazine) [kcal mol^{-1}]
A	0.00	3.3	−22.83	–[b]
B	1.44	−178.3	–[b]	−10.01
C	7.38	−90.8	−40.41	−32.46

[a] Conformer energies were computed with Gaussian 03 (DFT, B3LYP/6-31G(d,p)). ESP charges at the imidazole N2 and tetrazine N6 atoms were calculated with Spartan 04 (RHF/6-31G**). [b] Overlap with the electron density of the amide O atom that lies adjacent to the ring N atom gave an unrealistically high value of −65.16 (N2) and −59.14 kcal mol^{-1} (N6).

(−40.41 vs. −32.46 kcal mol^{-1}; see Supporting Information, Figure S3 for ESP maps). Hence, the intramolecular N–H···$N_{imidazole}$ interaction (in a five-membered ring) of conformer A should be stronger than the N–H···$N_{tetrazine}$ interaction (in a six-membered ring) of conformer B. Secondly, O_{amide}–$N_{imidazole}$ repulsion in conformer B (N8···O3: 2.82 Å) would be marginally more severe than O_{amide}–$N_{tetrazine}$ repulsion in conformer A (N6···O1: 2.96 Å). The marginally greater repulsion in conformer B could also be due to better overlap of the lone-pair orbitals of the heterocycle N and amide O atoms. Although the crystal lattice energy of form 3 is lower than that of forms 1 and 2 (Table 4), the strained conformer B destabilizes the total crystal energy of form 3. This situation, namely, a strained conformer stabilized in a lower-energy crystal environment, was found to be a general phenomenon in sets of conformational polymorphs analyzed recently.[16]

Table 4. Crystal-lattice energies[a] (U_{latt}) of TMZ polymorphs and cocrystals computed with Cerius^2 (COMPASS force field).

Crystal structure	T [K]	Conformer	U_{latt} [kcal mol^{-1}]
Form 2	100	A	−32.04
Form 1	100	A	−33.19
Form 1	298	A	−33.84
Form 3[b]	298	A+B	−34.17
Cocrystal I (1:0.5)	100	A	−33.27
Cocrystal II (2:1)	100	A	−30.32

[a] Per molecule. [b] The crystal structure of metastable form 3 could not be redetermined at 100 K because it is a disappearing polymorph.

As there are occasional exceptions to the density rule in polymorphs,[17] we verified the stability of polymorphs 1, 2, and 3 through energy computations as well as packing fractions (form 1: 74.9 %; form 2: 72.7 %; form 3: 70.5 %).

Temozolomide·4,4′-Bipyridine-*N*,*N*′-dioxide Cocrystals

Carboxylic acid and carboxamide dimer homosynthons are well-studied in crystal engineering.[5] Acid–pyridine and acid–amide heterosynthons (Scheme 3) have been profitably

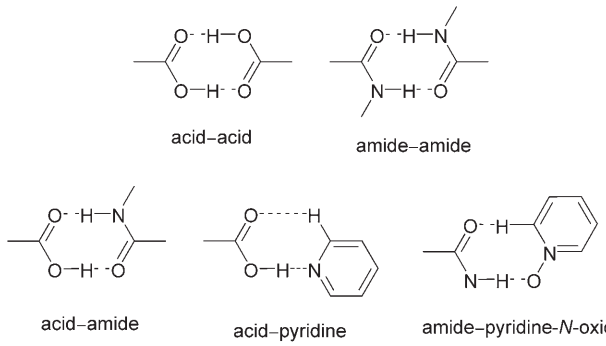

Scheme 3. Some common homo- and heterosynthons in crystal engineering.

exploited for the preparation of pharmaceutical cocrystals.[18] We showed that cocrystallization of amide-type drugs with pyridine-*N*-oxide partners (CCFs) gave crystal structures sustained by the amide–pyridine-*N*-oxide heterosynthon and/or amide dimer homosynthon.[19] The scope of this chemistry is extended through polymorphic TMZ·BPNO cocrystals of 1:0.5 and 2:1 composition (cocrystals I and II) and a 1:1 TMZ·BPNO cocrystal III.

TMZ·BPNO Cocrystal I

Cocrystallization of a 2:1 molar ratio of TMZ and BPNO from CH_3CN/EtOH afforded a 1:0.5 TMZ·BPNO crystalline adduct (cocrystal I, space group $P\bar{1}$). TMZ has conformation A, and BPNO resides on the inversion center. The amide *syn* N–H moiety interacts with the carbonyl acceptor of tetrazine through N1–H1A···O2 (2.10 and 3.085(2) Å, 164.4°), and the *anti* N–H moiety is bonded to the imidazole

N acceptor (N1−H1B···N2: 2.10 and 2.996(2) Å, 145.8°). With assistance from C4−H4···O2 interactions (2.33 and 3.398(2) Å, 166.4°), a 1D tape of TMZ dimers runs along the [001] direction. These TMZ tapes are sandwiched between ribbons of BPNO molecules to make a 2D sheet in the (210) plane (Figure 4). Surprisingly, neither the amide

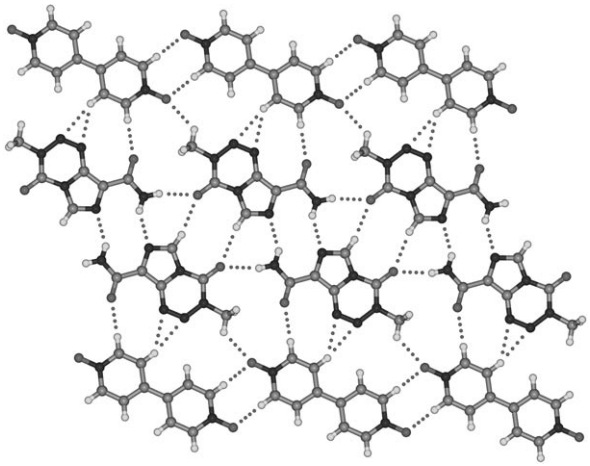

Figure 4. N−H···O and N−H···N hydrogen bonds between TMZ molecules and C−H···O interaction with BPNO in cocrystal I (1:0.5).

N−H···O homodimer nor the amide–pyridine-*N*-oxide heterosynthon (Scheme 3) is present in this crystal structure. The absence of these commonly observed synthons[19] suggests that there should be another polymorph.

TMZ·BPNO Cocrystal II

Cocrystallization in dimethyl sulfoxide (DMSO) by slow evaporation gave a 2:1 TMZ·BPNO cocrystal II in the space group $P2_1/c$. The chemical composition is the same as for cocrystal I except that the structure now contains two molecules of TMZ (conformer A) and one molecule of BPNO instead of one and half a molecule, respectively. Cocrystals I and II have the same molecular composition but different crystal-packing arrangements, that is, they are polymorphs of cocrystals.[20] There are 33 cocrystal-polymorph sets up to the January 2008 release of the CSD[9] (see Supporting Information, Table S1 for the refcodes), of which 24 structure sets have strongly hydrogen-bonding functional groups, and the remaining nine sets are sustained by weak C−H···O interactions or π–π stacking. In cocrystal II, the amide *syn* NH donors of crystallographically different TMZ molecules (shown as capped-stick and ball-and-stick models in Figure 5) undergo hydrogen bonding to the pyridine-*N*-oxide O acceptors of BPNO through N−H···O bonds (N1−H1A···O6: 1.81 and 2.826(1) Å, 177°; N7−H7A···O5: 1.84 and 2.851(2) Å, 172°). However, the *anti* NH moiety of one TMZ molecule makes no intermolecular contact, whereas the contact is long for the second molecule (N1−H1B···O6: 2.47 and 3.375(1) Å, 147.7°). Other weak interactions (C14−

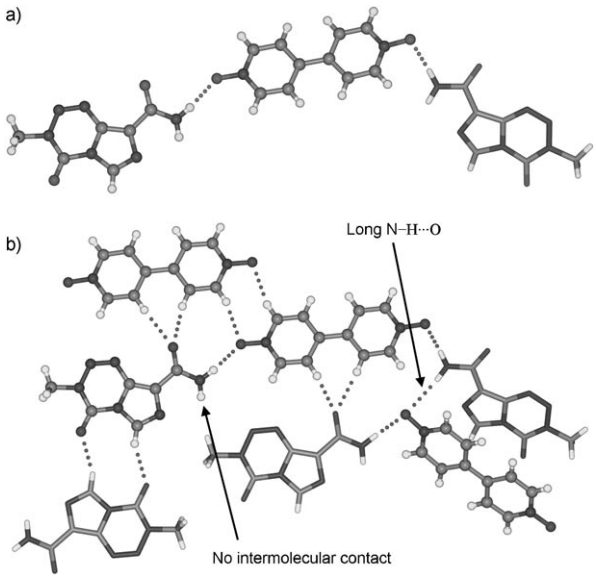

Figure 5. a) Amide–pyridine-*N*-oxide H bonds in cocrystal II (2:1). Symmetry-independent TMZ molecules are shown as capped-stick and ball-and-stick models. b) Packing in cocrystal II. One *anti* N−H···O bond is long (2.47 Å), whereas the other *anti* NH donor has intramolecular N−H···N interaction only.

H14···O1: 2.06 and 3.129(1) Å, 168.5°; C19−H19···O1: 2.31 and 3.396(1) Å, 173.8°) are listed in Table 2.

TMZ·BPNO Cocrystal III

Besides polymorphic cocrystal structures I and II, a 1:1 TMZ·BPNO cocrystal III was obtained from *N*,*N*-dimethylformamide (DMF) in the chiral space group $P2_12_12_1$. BPNO forms a linear 1D ribbon of C−H···O dimers (C12−H12···O3: 2.17 and 3.240(7) Å, 167.8°; C7−H7···O4: 2.11 and 3.195(7) Å, 173.5°). A TMZ molecule is bonded to one of the *N*-oxides from the amide *syn* NH bond (N1−H1A···O3: 1.86 and 2.857(6) Å, 167.2°). The crystal structure has alternating tapes of TMZ and BPNO molecules in a 2D sheet (Figure 6). Here, too, the amide *anti* NH moiety has no intermolecular contact. Cocrystal III is a layered structure (similar to cocrystal I) and contains alternate tapes of TMZ and BPNO linked by the amide–pyridine-*N*-oxide H bond.

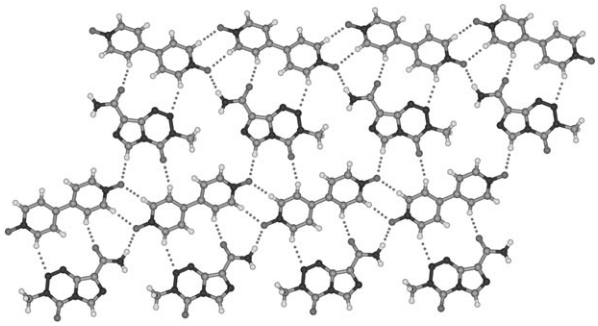

Figure 6. Amide–pyridine-*N*-oxide H bonds in cocrystal III (1:1). There are alternate tapes of TMZ and BPNO molecules in the 2D sheet structure. The *anti* NH donor makes an intramolecular N−H···N interaction.

CHEMISTRY
AN ASIAN JOURNAL

In comparison, cocrystal I has linear tapes of TMZ dimers sandwiched between ribbons of BPNOs in a 2D sheet. The amide *anti* NH moiety was often found not to make intermolecular contacts because it is a weaker hydrogen-bond donor than the *syn* NH moiety of primary amides.[21]

A likely reason for cocrystallization in multiple compositions of 1:0.5, 2:1, and 1:1 is the presence of different N/O acceptor groups in temozolomide. The amide *syn* NH moiety bonds to the temozolomide C=O group or the pyridine-*N*-oxide O atom, and there are differences in *anti* NH bonding (Figures 4–6). An issue that remains to be addressed in cocrystals I–III is that they are not classified as pharmaceutical cocrystals[2f,4a] because of the BPNO component. Cocrystallization of TMZ with GRAS (generally regarded as safe) molecules and excipients that contain carboxylic acid or carboxamide functional groups is a potential pharmaceutical solution.[22]

Grinding Experiments

There has been renewed interest in mechanochemistry.[23] When cocrystal II was ground in a ball mill for 1 h, it was completely converted into cocrystal I, according to comparison of the PXRD data. Further grinding of cocrystal I did not indicate any phase change, which suggests that cocrystal I is more stable than II (Figures 7 and 8). The metastable nature of cocrystal II may be traced to the unused NH donor in intermolecular hydrogen bonding.

The density of cocrystal I is higher than that of II (1.592, 1.576 $g\,cm^{-3}$, respectively; packing fraction: 74.1, 73.2%, respectively). Lattice-energy (Table 4) calculations place cocrystal I ($-33.27\ kcal\,mol^{-1}$) as substantially more stable than II ($-30.32\ kcal\,mol^{-1}$), given that energy differences between polymorphs are generally small. It is difficult to infer cocrystal stability from melting points because of compound decomposition. Attempts to determine the stability of the cocrystal forms as a function of temperature were frustrated by the decomposition of the BPNO component. Solution-mediated transformations and a study into the effect of ultrasound on phase transitions are under way.

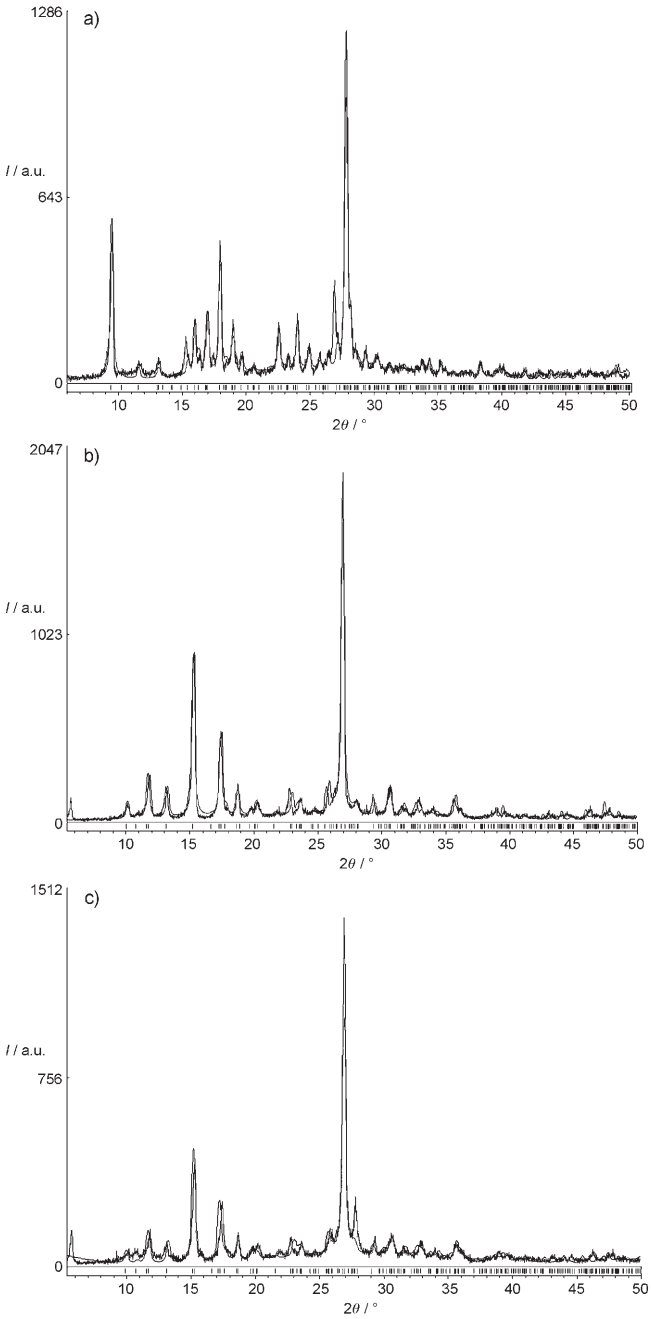

Figure 7. Powder X-ray diffraction patterns. a) Freshly prepared cocrystal II (100% purity). b) Pure cocrystal II ground in a mechanical ball mill for 1 h, showing a quantitative transformation into cocrystal I. c) Further grinding for 1 h showed no change (cocrystal I recovered). These phase transitions indicate that cocrystal I is the thermodynamic phase and cocrystal II is a metastable polymorph. The black trace is the experimental PXRD, and the gray lines were simulated from the X-ray crystal structure. The observed and calculated peaks match well. The small shift in 2θ values between the observed and calculated lines is because the powder diffraction was recorded at 300 K but the X-ray crystal structures were determined at 100 K.

Synthon Polymorphism

Supramolecular-synthon-based polymorphism, or synthon polymorphism, has been reported in the literature.[24,8a,20a] A few common examples of synthon polymorphs are sulfathiazole,[25] isonicotinamide,[8b] and tetrolic acid.[26] Differences arise due to different hydrogen-bond synthons.[27] Polymorphic crystal structures of hydrogen-bonding functional groups may be analyzed at two levels: the primary level of the cyclic synthon or strong H bonds and the secondary level of single H bonds or weak interactions. Crystal structures I–III have different primary synthons. Cocrystal I has tapes of amide N–H···O bonds and N–H···N dimers, whereas cocrystal II has amide–pyridine-*N*-oxide synthons. The *anti* NH moiety engages in N–H···N bonds in I, whereas it makes long N–H···O contacts and no intermolecular H bond in the two symmetry-independent molecules of cocrystal II. The weaker TMZ C–H···O dimer and BPNO C–H···O dimer are present in both crystal structures; they are similar at the secondary-synthon level. Cocrystal III (1:1) is exclud-

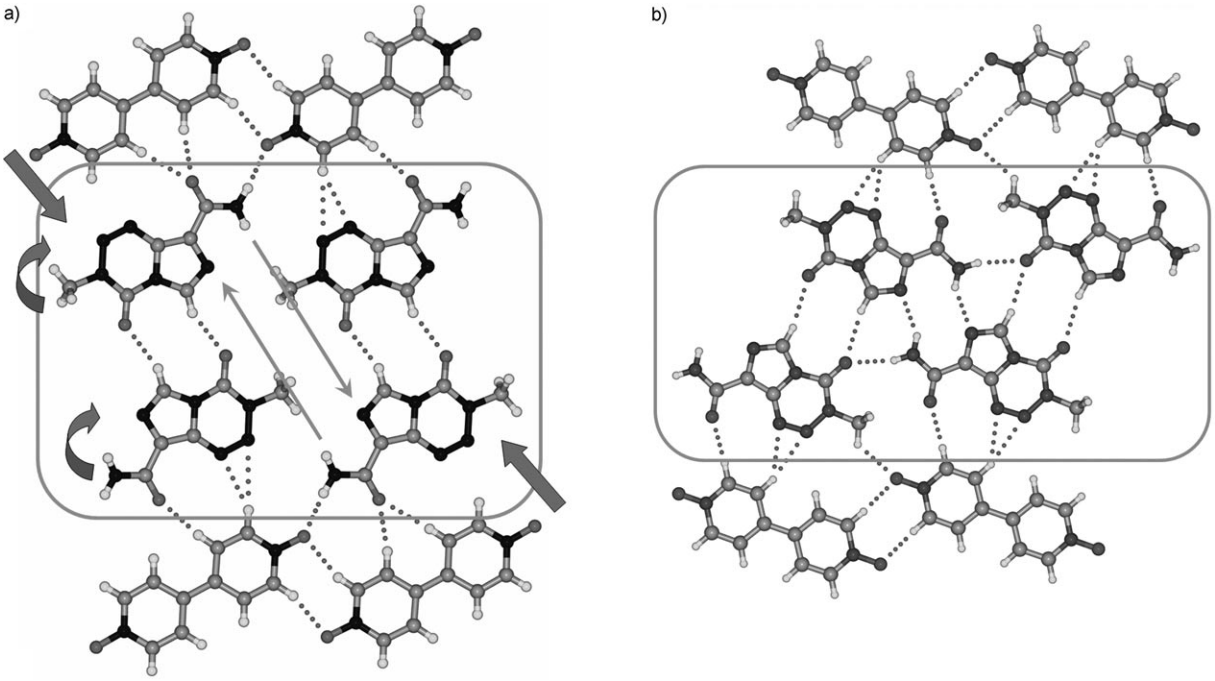

Figure 8. Hydrogen-bond reorganization in TMZ·BPNO cocrystal II (2:1; a) to cocrystal I (1:0.5; b). Cocrystal II has a strong amide–pyridine-*N*-oxide N–H···O bond. The unused amide *anti* N–H donors in cocrystal II (a); see thin double arrows) move close to the imidazole N acceptors in cocrystal I (b) by 45° rotation and a translation of about half a molecular length. One strong N–H···O bond is broken and replaced by N–H···O and N–H···N bonds. Molecular rotation and translation in a) are indicated by thick arrows.

ed as it is not polymorphic to I and II. Polymorphs 1, 2, and 3 have the same amide dimer of the $R^2_2(8)$ graph set,[28] but the *anti* NH moieties make different intermolecular interactions: N–H···O and N–H···N in form 1, no short contact in form 2, and N–H···N in form 3. To summarize, the primary N–H···O dimer synthon is the same in TMZ polymorphs, but the secondary N–H···N/N–H···O hydrogen bonds are different. In contrast, the primary synthon is different in the cocrystals, but the secondary C–H···O synthons are the same. Synthon comparisons for Figures 1–5 are summarized in Scheme 4 (see also Supporting Information, Figure S4).

The identification of unused hydrogen-bond donors/acceptors in crystal structures has attracted special mention.[29] Etter[30] proposed hydrogen-bonding rules in molecular crystals. The first rule states that "all good proton donors and acceptors are used in hydrogen bonding." Thus, molecules with strong donors, such as O–H, N–H, and C=O acceptor are expected to form conventional hydrogen bonds. Alloxan is the archetypal amide with strong NH donors and C=O acceptors, but these groups hardly engage in conventional hydrogen bonds.[29b,c,e] When such strong hydrogen bonds are absent, the acceptor may seek out C–H donors to form weak hydrogen bonds.[29d] Carbamazepine polymorphs are sustained by the persistent amide dimer, but the *anti* NH donor is not involved in intermolecular H bonding owing to the geometric constraint of the dibenzapine ring[31] and the absence of other heteroatom acceptors in the molecule.

The analysis of crystal structures as synthon polymorphs is helpful in explaining polymorph stabilities. The facile

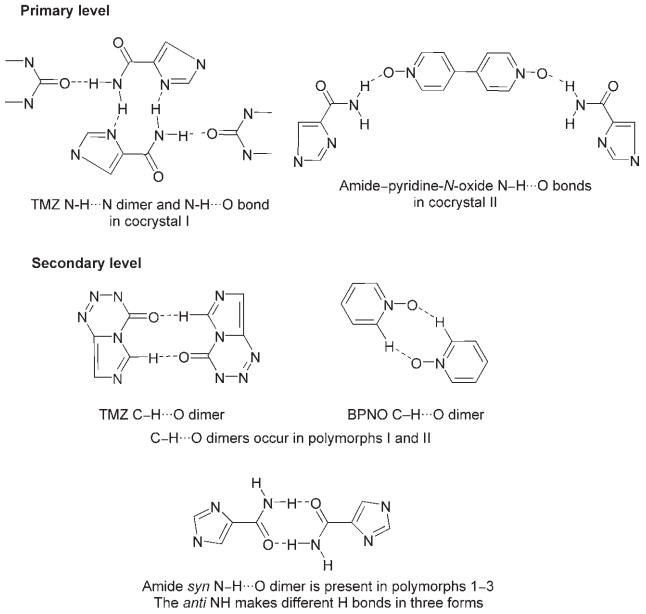

Scheme 4. Synthon polymorphism in temozolomide polymorphs 1–3 and cocrystals I and II. Molecular fragments are truncated. See Supporting Information, Figure S4 for secondary synthons in TMZ forms 1–3.

phase transition of TMZ·BPNO cocrystal II to I upon grinding may be understood by stabilization owing to the greater number of hydrogen bonds in the product. Although the amide–pyridine-*N*-oxide N–H···O bond in structure II (1.81

CHEMISTRY
AN ASIAN JOURNAL

and 1.84 Å) is quite strong (more stable than amide N–H···O by ≈3 kcal mol^{-1}),[19] the unutilized *anti* NH donor and heterocycle N acceptor make the crystal structure kinetically metastable. The single strong N–H···O bond in structure II is replaced by two H bonds in I: N–H···O with the tetrazine C=O group and N–H···N with the imidazole N atom (Figure 8). Similarly, the unused *anti* NH donor in metastable TMZ form 2 participates in an intermolecular N–H···O bond in form 1 after molecular reorganization (Figure 9). The helical architecture persists before and after reorganization (see Supporting Information, Figure S5). Form 1 is more stable than 2 by 1.15 kcal mol^{-1}, and cocrystal I is lower in energy than II by 2.95 kcal mol^{-1} (Table 4).

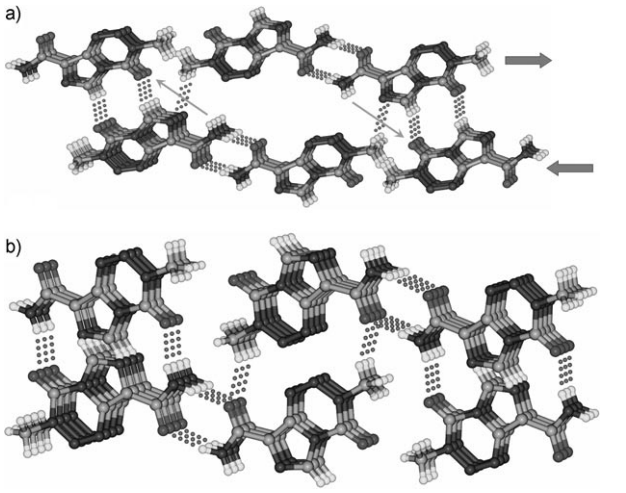

Figure 9. Hydrogen-bond reorganization of form 2 (a) to form 1 of TMZ (b). The unused amide *anti* N–H moiety in form 2 (a); thin arrows) undergoes a translation of half a molecular length to make an intermolecular N–H···O bond in form 1 (b). This pathway accounts for the major and minor composition of forms 1 and 2 in concomitant crystallization. See also Supporting Information, Figure S5.

Dimorphs of the pigment 2,9-dichloro-5,12-dihydroquino-(2,3-b)acridine-7,14-dione[32] typify a similar situation. Two unused NH donors and C=O acceptors in the black polymorph (−50.26 kcal mol^{-1}, Cerius^2) make N–H···O bonds in the red form (−59.93 kcal mol^{-1}). All these cases characterize unused/partially used donors/acceptors in the metastable structure and maximal intermolecular hydrogen bonding in the stable modification. The potential of synthon classification for polymorphs goes beyond structural analysis to the understanding and control of crystallization. The dimer and catemer synthons of tetrolic acid in the solid state are related to the corresponding structural motifs in solution.[26b] Crystallization of metastable form I sulfathiazole is promoted in the presence of *N*-acetylsulfathiazole because the additive inhibits the growth of forms II–IV (synthon mimicry).[25b]

Conclusions

X-ray crystal structures of three polymorphs and three cocrystals of temozolomide are reported. Only one crystal structure of TMZ and no cocrystals were known prior to this study. A new strained conformer B of temozolomide is isolated as form 3, but the crystallization could not be reproduced because it is a disappearing polymorph. Crystal-structure analysis as synthon polymorphs at the primary and secondary level highlights similarities and differences in their hydrogen bonding. The crystal-form stability determined in experiments and computations is consistent with hydrogen-bond-reorganization pathways that utilize unused donors/acceptors in the metastable form to make intermolecular hydrogen bonds in the stable polymorph. Our results show that structural relationships in the growing subset of polymorphic cocrystals[33] are of similar origin to those of the well-studied molecular polymorphs.

Experimental Section

Preparation of Polymorphs and Cocrystals

Temozolomide was supplied by Dabur Research Foundation, India. Crystallization of TMZ from common solvents such as EtOH, *i*PrOH, acetone, and CH_3CN by slow evaporation resulted in single crystals of the known monoclinic form 1.[6] Attempted cocrystallization with CBZ in a 1:1 molar ratio (TMZ: 25 mg, 0.127 mmol; CBZ: 30 mg, 0.127 mmol) by dissolving the components in EtOH (5 mL) followed by slow evaporation of the solvent gave single crystals. The needle-shaped crystals had a monoclinic unit cell, and a few irregularly shaped crystals were triclinic. The observed cell parameters are different from the known crystal structure, and we designated these polymorphs as forms 2 and 3 (Table 1). Attempts to reproduce form 3 (disappearing polymorph)[15] gave a concomitant mixture of form 1 (plate or block morphology, dominant) and form 2 (needle-shaped, minor) but no form 3. Form 2 was also obtained by cocrystallization of TMZ and 3-hydroxypyridine-*N*-oxide in MeOH. No cocrystals were obtained in these experiments.

Cocrystals were prepared with the BPNO partner molecule.[19] The stoichiometry was determined by the functional-group ratio of the binary system. Cocrystallization of a 2:1 molar mixture of TMZ (50 mg, 0.257 mmol) and BPNO dihydrate (27 mg, 0.128 mmol) in CH_3CN/EtOH (3:1) gave cocrystal I of TMZ·BPNO (1:0.5). A novel hydrate form of TMZ appeared concomitantly (see Supporting Information, Figure S6).[34] When the crystallization solvent was changed to DMSO, cocrystal II resulted (2:1), with a different space group (Table 1). Larger batches of cocrystal II were prepared by ultrasonication[35] of a 2:1 molar mixture of TMZ and BPNO in MeOH (5 mL) for 5 min. A third cocrystal (III) of 1:1 stoichiometry was obtained by cocrystallization of TMZ (50 mg, 0.24 mmol) and BPNO dihydrate (52 mg, 0.24 mmol) from DMF (5 mL).

X-ray Crystal Structures

Reflections on single crystals of TMZ polymorphs and cocrystals were collected on a Bruker SMART-APEX CCD X-ray diffractometer ($Mo_{K\alpha}$ radiation, $\lambda = 0.71073$ Å). SMART was used for collecting frames, indexing reflections, and determining lattice parameters. The integration of reflection intensity and scaling was carried out with SAINT. Absorption correction was done with SADABS,[36] and SHELX-TL[37] was used for space-group determination, structure solution, and least-squares refinement on F^2 to give a satisfactory R factor (Table 1). Structures were solved by direct methods. Amide hydrogen atoms were located in difference electron density Fourier maps and refined isotropically. Non-hydrogen atoms were refined anisotropically. CH hydrogen atoms were generated geometrically and allowed to ride on the bound heavy atom. X-

Seed[38] was used to prepare the figures and packing diagrams. CCDC-665056 (TMZ monohydrate), -665057 (TMZ BPNO cocrystal I), -665058 (TMZ BPNO cocrystal II), -665059 (TMZ BPNO cocrystal III), -665060 (TMZ form 1), -665061 (TMZ form 2), and -665062 (TMZ form 3) contain the supplementary crystallographic data for this paper. These data can be obtained free of charge from The Cambridge Crystallographic Data Centre at www.ccdc.cam.ac.uk/data_request/cif.

Powder X-ray Diffraction

PXRD was performed on a PANalytical 1830 (Philips Analytical) diffractometer with $Cu_{K\alpha}$ X-radiation ($\lambda = 1.54056$ Å) at 35 kV power and 25 mA current over the 2θ range 5–50° at a scan rate of $1° min^{-1}$. The Powder Cell 2.3 program[39] was used for the least-squares refinement and to generate calculated diffraction patterns from the X-ray crystal structures.

Solid-State Grinding

Cocrystal II (75 mg) was ground in a ball mill for 60 min. The sample was shaken in a Wig-L-Bug-type mixer mill equipped with a 5-mL stainless-steel grinding jar and balls 4 mm in diameter. Grinding was performed at an oscillation rate of 20 Hz. PXRD showed that cocrystal II was completely converted into cocrystal I. When cocrystal I was ground in a ball mill for 60 min, there was no visible change in the diffraction pattern.

Computations

Conformer energies were calculated with Gaussian 03 (DFT, B3LYP/6-31G(d,p)).[40] As the observed conformation in the crystal structure is usually different from the gas-phase-minimized conformer and often higher in energy, constrained optimization of the crystal conformer was carried out by keeping the main torsion angles fixed but allowing the bond lengths/distances and angles to relax at the nearest local minima (E_{conf}).[16] Lattice energies were computed in Cerius^2 with the COMPASS force field.[41] Crystal structures were minimized (U_{latt}) by allowing small variations in cell parameters but not gross differences between the calculated and experimental crystal lattice. The electrostatic potential map of the conformers A and B as well as the perpendicular amide conformation C were computed with Spartan 04[42] (RHF/6-31G**; see Supporting Information, Figure S3).

Cambridge Structural Database

The CSD[9] (version 5.29, November 2007, ConQuest 1.10, January 2008 update) was searched for cocrystal polymorphs. The parameters "all polymorphic structures with 3D coordinates determined", "no errors", "no polymeric", and "no ions" were searched to give 5167 hits. The crystal structures were visualized with Mercury 2.0, and 33 sets of cocrystal polymorphs were manually retrieved (3D coordinates reported for all polymorph sets). Crystal structures with a high degree of disorder were excluded. Of the 33 sets, 24 have strongly hydrogen-bonding groups, whereas nine do not contain such groups but instead have weak intermolecular interactions and/or π stacking. Details of polymorphic cocrystal sets are listed in the Supporting Information, Table S1.

Acknowledgements

We thank the DST (SR/S1/RFOC-01/2007) and CSIR (01(2079)/06/EMR-II) for funding. UGC and CSIR provided fellowships to N.J.B., L.S.R., and S.A. DST (IRPHA) funded the CCD X-ray diffractometer, and the CMSD-HPC facility is supported by DST-UPE. We are grateful to UGC for the UPE program and Dabur Research Foundation for their interest in this project.

[1] a) J. Bernstein, *Polymorphism in Molecular Crystals*, Clarendon, Oxford, **2002**; b) *Polymorphism in the Pharmaceutical Industry* (Ed.: R. Hilfiker), Wiley-VCH, Weinheim, **2006**; c) Special Section on Facets of Polymorphism in Crystals (Guest Ed.: A. J. Matzger): *Cryst. Growth Des.* **2008**, *8*, 2–161.

[2] a) P. Vishweshwar, J. A. McMahon, M. J. Zaworotko in *Frontiers in Crystal Engineering* (Eds.: E. R. T. Tiekink, J. J. Vittal), Wiley, Chichester, **2006**, pp. 25–49; b) J. F. Remenar, S. L. Morissette, M. L. Peterson, B. Moulton, J. M. MacPhee, H. R. Guzman, Ö. Almarsson, *J. Am. Chem. Soc.* **2003**, *125*, 8456; c) D. P. McNamara, S. L. Childs, J. Giordano, A. Iarriccio, J. Cassidy, M. S. Shet, R. Mannion, E. O'Donnell, A. Park, *Pharm. Res.* **2006**, *23*, 1888; d) M. B. Hickey, M. L. Peterson, L. A. Scoppettuolo, S. L. Morrisette, A. Vetter, H. Guzmán, J. F. Remenar, Z. Zhang, M. D. Tawa, S. Haley, M. J. Zaworotko, Ö. Almarsson, *Eur. J. Pharm. Biopharm.* **2007**, *67*, 112; e) Special Section on Pharmaceutical Cocrystals (Guest Ed.: N. Rodríguez-Hornedo): *Mol. Pharm.* **2007**, *4*, 299–434.

[3] a) B. Rodríguez-Spong, C. P. Price, A. Jayashankar, A. J. Matzger, N. Rodríguez-Hornedo, *Adv. Drug Delivery Rev.* **2004**, *56*, 241; b) G. P. Stahly, *Cryst. Growth Des.* **2007**, *7*, 1007; c) A. V. Trask, *Mol. Pharm.* **2007**, *4*, 301.

[4] a) Ö. Almarsson, M. J. Zaworotko, *Chem. Commun.* **2004**, 1889; b) C. B. Aakeröy, D. J. Salmon, *CrystEngComm* **2005**, *7*, 439.

[5] G. R. Desiraju, *Angew. Chem.* **1995**, *107*, 2541; *Angew. Chem. Int. Ed. Engl.* **1995**, *34*, 2311.

[6] P. R. Lowe, C. E. Sansom, C. H. Schwalbe, M. F. G. Stevens, A. S. Clark, *J. Med. Chem.* **1992**, *35*, 3377.

[7] I. Adin, C. Iustain, Novel Crystalline Forms of Temozolomide, US Patent 2005/0187206A1, **2005**; the nine forms are numbered I–IX.

[8] a) A. Nangia, G. R. Desiraju, *Top. Curr. Chem.* **1998**, *198*, 57; b) C. B. Aakeröy, A. M. Beatty, B. A. Helfrich, M. Nieuwenhuyzen, *Cryst. Growth Des.* **2003**, *3*, 159.

[9] Cambridge Structural Database (version 5.29), November 2007, ConQuest 1.10, January 2008 update, The Cambridge Crystallographic Data Centre, Cambridge (UK), to be found under www.ccdc.cam.ac.uk.

[10] a) C. B. Aakeröy, A. Beatty, B. A. Helfrich, *Angew. Chem.* **2001**, *113*, 3340; *Angew. Chem. Int. Ed.* **2001**, *40*, 3240; b) C. B. Aakeröy, J. Desper, B. A. Helfrich, *CrystEngComm* **2004**, *6*, 19; c) J. A. McMahon, J. A. Bis, P. Vishweshwar, T. R. Shattock, O. L. McLaughlin, M. J. Zaworotko, *Z. Kristallogr.* **2005**, *220*, 340; d) B. R. Bhogala, S. Basovaju, A. Nangia, *CrystEngComm* **2005**, *7*, 551.

[11] J. W. Steed, *CrystEngComm* **2003**, *5*, 169.

[12] a) C. Bilton, J. A. K. Howard, N. N. L. Madhavi, A. Nangia, G. R. Desiraju, F. Allen, C. C. Wilson, *Chem. Commun.* **1999**, 1675; b) V. S. S. Kumar, A. Addlagatta, A. Nangia, W. T. Robinson, C. K. Broder, R. Mondal, I. R. Evans, J. A. K. Howard, F. H. Allen, *Angew. Chem.* **2002**, *114*, 4004; *Angew. Chem. Int. Ed.* **2002**, *41*, 3848; c) Z.-Q. Zhang, J. N. Njus, D. J. Sandman, C. Guo, B. H. Foxman, P. Erk, R. van Gelder, *Chem. Commun.* **2004**, 886.

[13] Aspirin: a) P. Vishweshwar, J. A. McMahon, M. Oliveira, M. L. Peterson, M. J. Zaworotko, *J. Am. Chem. Soc.* **2005**, *127*, 16802; maleic acid: b) G. M. Day, A. V. Trask, W. D. S. Motherwell, W. Jones, *Chem. Commun.* **2006**, 54; benzidine: c) M. Rafilovich, J. Bernstein, *J. Am. Chem. Soc.* **2006**, *128*, 12185.

[14] A. Burger, R. Ramberger, *Mikrochim. Acta* **1979**, *2*, 273.

[15] J. D. Dunitz, J. Bernstein, *Acc. Chem. Res.* **1995**, *28*, 193.

[16] A. Nangia, *Acc. Chem. Res.* **2008**, *41*, 595

[17] The most dense polymorph is not always the thermodynamic form: H. H. Y. Tong, B. Y. Shekunov, J. P. Chan, C. K. F. Mok, H. C. M. Hung, A. H. L. Chow, *Int. J. Pharm.* **2005**, *295*, 191.

[18] Acid–pyridine: a) R. D. B. Walsh, M. W. Bradner, S. Fleishman, L. A. Morales, B. Moulton, N. Rodríguez-Hornedo, M. J. Zaworotko, *Chem. Commun.* **2003**, 186; b) B. R. Bhogala, A. Nangia, *Cryst. Growth Des.* **2003**, *3*, 547; c) A. V. Trask, W. D. S. Motherwell, W. Jones, *Cryst. Growth Des.* **2005**, *5*, 1013; amide–acid: d) P. Vishweshwar, J. A. McMahon, J. A. Bis, M. J. Zaworotko, *J. Pharm. Sci.* **2006**, *95*, 499.

[19] Amide–pyridine-*N*-oxide: a) L. S. Reddy, N. J. Babu, A. Nangia, *Chem. Commun.* **2006**, 1369; b) N. J. Babu, L. S. Reddy, A. Nangia, *Mol. Pharm.* **2007**, *4*, 417.

[20] a) B. R. Sreekanth, P. Vishweshwar, K. Vyas, *Chem. Commun.* **2007**, 2375; b) J. A. Bis, P. Vishweshwar, R. A. Middleton, M. J. Zaworotko, *Cryst. Growth Des.* **2006**, *6*, 1048; c) S. L. Childs, K. I. Hardcastle, *Cryst. Growth Des.* **2007**, *7*, 1291; d) J. A. Bis, P. Vishweshwar, D. Weyna, M. J. Zaworotko, *Mol. Pharm.* **2007**, *4*, 401; e) W. W. Porter III, S. C. Elie, A. J. Matzger, *Cryst. Growth Des.* **2008**, *8*, 14.

[21] K. Kobayashi, A. Sato, S. Sakamoto, K. Yamaguchi, *J. Am. Chem. Soc.* **2003**, *125*, 3035.

[22] The GRAS chemicals list is available at http://www.cfsan.fda.gov/~dms/eafus.html; pharmaceutical cocrystals of TMZ with GRAS acids and amides have been prepared (manuscript in preparation).

[23] a) L. S. Reddy, P. M. Bhatt, R. Banerjee, A. Nangia, G. J. Kruger, *Chem. Asian J.* **2007**, *2*, 505; b) A. V. Trask, W. Jones, *Top. Curr. Chem.* **2005**, *254*, 41; c) N. J. Babu, A. Nangia, *CrystEngComm* **2007**, *9*, 980; d) A. V. Trask, N. Shan, W. D. S. Motherwell, W. Jones, S. Feng, R. B. H. Tan, K. J. Carpenter, *Chem. Commun.* **2005**, 880.

[24] R. K. R. Jetti, R. Boese, J. A. R. P. Sarma, L. S. Reddy, P. Vishweshwar, G. R. Desiraju, *Angew. Chem.* **2003**, *115*, 2008; *Angew. Chem. Int. Ed.* **2003**, *42*, 1963.

[25] a) N. Blagden, R. J. Davey, H. F. Lieberman, L. Williams, R. Payne, R. Roberts, R. Rowe, R. Docherty, *J. Chem. Soc. Faraday Trans.* **1998**, *94*, 1035; b) J. M. Kelleher, S. E. Lawrence, H. A. Moynihan, *CrystEngComm* **2006**, *8*, 327.

[26] a) V. Benghiat, A. Gavezzotti, *J. Chem. Soc. Perkin Trans. 2* **1972**, 1763; b) S. Parveen, R. J. Davey, G. Dent, R. G. Pritchard, *Chem. Commun.* **2005**, 1531; c) A. J. Florence, K. Shakland, T. Gelbrich, M. B. Hurthouse, N. Shakland, A. J. Johnston, P. Fernandes, C. K. Leech, *CrystEngComm* **2008**, *10*, 26.

[27] Sulfathiazole[25a] form I has the $R^2_2(8)$ motif of N–H···N, whereas forms II–IV have the $R^2_2(18)$ motif of N–H···N and N–H···O bonds. Isonicotinamide[8b] has the N–H···O bond in one polymorph and N–H···N in the other, tetrolic acid[26b] dimorphs differ by the COOH dimer and catemer O–H···O synthons, and cyheptamide[26c] (an analogue of carbamazepine) dimorphs have dimer and catemer N–H···O synthons.

[28] J. Bernstein, R. E. Davis, L. Shimoni, N.-L. Chang, *Angew. Chem.* **1995**, *107*, 1689; *Angew. Chem. Int. Ed. Engl.* **1995**, *34*, 1555.

[29] a) G. R. Desiraju, *CrystEngComm* **2002**, *4*, 499; b) J. D. Dunitz, W. B. Schweizer, *CrystEngComm* **2007**, *9*, 266; c) T. C. Lewis, D. A. Tocher, S. L. Price, *Cryst. Growth Des.* **2005**, *5*, 983; d) L. S. Reddy, S. K. Chandran, S. George, N. J. Babu, A. Nangia, *Cryst. Growth Des.* **2007**, *7*, 2675; e) R. M. Ibberson, W. G. Marshall, L. E. Budd, S. Parsons, C. R. Pulham, C. K. Spanswick, *CrystEngComm* **2008**, *79*, 183. A second form of alloxan[29e] has shorter N–H···O bonds, but the distance is still >2.0 Å.

[30] a) M. C. Etter, *Acc. Chem. Res.* **1990**, *23*, 120; b) M. C. Etter, *J. Phys. Chem.* **1991**, *95*, 4601.

[31] A. L. Grzesiak, M. Lang, K. Kim, A. J. Matzer, *J. Pharm. Sci.* **2003**, *92*, 2260.

[32] a) T. Senju, T. Hoki, J. Mizuguchi, *Acta Crystallogr. Sect. E* **2005**, *61*, o1061; b) T. Senju, N. Nishimura, T. Hoki, J. Mizuguchi, *Acta Crystallogr. Sect. E* **2005**, *61*, o2596; c) N. Panina, R. van de Ven, P. Verwer, H. Meekes, E. Vlieg, G. Deroover, *Dyes Pigments* **2008**, *79*, 183.

[33] The total number of polymorph sets (neutral, organic compounds) was estimated at around 1600 in 2007,[16] as opposed to over 30 cocrystal polymorph sets today (see Supporting Information, Table S1).

[34] Needle- to block-shaped TMZ monohydrate crystals were obtained concomitantly with cocrystal I. The structure was solved as being in the monoclinic space group $P2_1/m$ with unit-cell dimensions $a=7.5134(9)$, $b=6.3187(7)$, $c=9.5330(11)$ Å, $\beta=92.868(2)°$, $V=452.01(9)$ Å^3, $Z=2$, $\rho_{calcd}=1.559$ g cm^{-3}, $R1=0.0385$, $wR2=0.1026$.

[35] D.-K. Buèar, L. R. MacGillivray, *J. Am. Chem. Soc.* **2007**, *129*, 32.

[36] G. M. Sheldrick, SADABS, Program for Empirical Absorption Correction of Area Detector Data, University of Göttingen, Göttingen (Germany), **1997**.

[37] G. M. Sheldrick, SHELXS-97 and SHELXL-97, Programs for the Solution and Refinement of Crystal Structures, University of Göttingen, Göttingen (Germany), **1997**.

[38] L. J. Barbour, X-Seed, Graphical Interface to SHELX-97 and POV-Ray, University of Missouri, Columbia, MO (USA), **1999**.

[39] Rietveld refinement was carried out with Powder Cell: N. Kraus, G. Nolze, Powder Cell (version 2.3), Federal Institute for Materials Research and Testing, Berlin (Germany), **2000**.

[40] Gaussian 03 (Revision B.05), M. J. Frisch, G. W. Trucks, H. B. Schlegel, G. E. Scuseria, M. A. Robb, J. R. Cheeseman, J. A. Montgomery, Jr., T. Vreven, K. N. Kudin, J. C. Burant, J. M. Millam, S. S. Iyengar, J. Tomasi, V. Barone, B. Mennucci, M. Cossi, G. Scalmani, N. Rega, G. A. Petersson, H. Nakatsuji, M. Hada, M. Ehara, K. Toyota, R. Fukuda, J. Hasegawa, M. Ishida, T. Nakajima, Y. Honda, O. Kitao, H. Nakai, M. Klene, X. Li, J. E. Knox, H. P. Hratchian, J. B. Cross, C. Adamo, J. Jaramillo, R. Gomperts, R. E. Stratmann, O. Yazyev, A. J. Austin, R. Cammi, C. Pomelli, J. W. Ochterski, P. Y. Ayala, K. Morokuma, G. A. Voth, P. Salvador, J. J. Dannenberg, V. G. Zakrzewski, S. Dapprich, A. D. Daniels, M. C. Strain, O. Farkas, D. K. Malick, A. D. Rabuck, K. Raghavachari, J. B. Foresman, J. V. Ortiz, Q. Cui, A. G. Baboul, S. Clifford, J. Cioslowski, B. B. Stefanov, G. Liu, A. Liashenko, P. Piskorz, I. Komaromi, R. L. Martin, D. J. Fox, T. Keith, M. A. Al-Laham, C. Y. Peng, A. Nanayakkara, M. Challacombe, P. M. W. Gill, B. Johnson, W. Chen, M. W. Wong, C. Gonzalez, J. A. Pople, Gaussian, Inc., Pittsburgh PA, **2003**

[41] Cerius^2, Materials Studio, to be found under www.accelrys.com.

[42] Spartan 04, to be found under www.wavefun.com.

Received: March 4, 2008
Published online: June 2, 2008

